

Carbon Nanotube Yarn-Based Glucose Sensing Artificial Muscle

Junghan Lee, Sachan Ko, Cheong Hoon Kwon, Márcio D. Lima, Ray H. Baughman, and Seon Jeong Kim*

Boronic acid (BA), known to be a reversible glucose-sensing material, is conjugated to a nanogel (NG) derived from hyaluronic acid biopolymer and used as a guest material for a carbon multiwalled nanotube (MWNT) yarn. By exploiting the swelling/deswelling of the NG that originates from the internal anionic charge changes resulting from BA binding to glucose, a NG MWNT yarn artificial muscle is obtained that provides reversible torsional actuation that can be used for glucose sensing. This actuator shows a short response time and high sensitivity (in the $5\text{--}100 \times 10^{-3}$ M range) for monitoring changes in glucose concentration in physiological buffer, without using any additional auxiliary substances or an electrical power source. It may be possible to apply the glucose-sensing MWNT yarn muscles as implantable glucose sensors that automatically release drugs when needed or as an artificial pancreas.

1. Introduction

Glucose monitoring is very important for determining the optimal medical treatment for patients suffering from diabetes due to insulin deficiency.^[1,2] For the continuous measurement of blood glucose levels, there have been many advances in continuous glucose monitoring technology using various glucose sensitive materials.^[3–5] Among them, glucose oxidase (GOx)-based sensors showed impressive results, yet they have some difficulties to overcome. Enzymes are very sensitive to the environment and are susceptible to denaturation. The GOx sensor requires oxygen or another redox mediator, consumes glucose, and produces H_2O_2 .^[6,7]

Recently, boronic acid (BA) has been of interest for alternative glucose sensors, due to its reversible binding with glucose as a nonenzymatic glucose sensing material.^[8,9] Various studies have provided interesting results, but there are problems to overcome, such as detection limits using fluorescent probes, demonstration of safe use in the human body, and the need for means for directly converting sensor detection to actuation without use of an external energy source.^[10,11]

We previously synthesized multiwalled carbon nanotube (MWNT) sheets and yarns from special MWNT forests from which carbon nanotubes can be continuously drawn.^[12] These MWNT sheets or yarns are of great interest for application as artificial muscles because of their strength, electronic conductivity, and high accessible surface area.^[13] MWNT yarns, including those containing guest materials, have been intensively studied for physical and chemical applications including superconductors, lithium-ion battery materials, graphene ribbons, catalytic nanofibers for fuel cells, and photocatalysis.^[14–16] However, to the best of our knowledge, there have been almost no reports of the use of MWNT yarn as materials that actuate in response to external influences like pH, ionic strength, antigens, and enzymes.

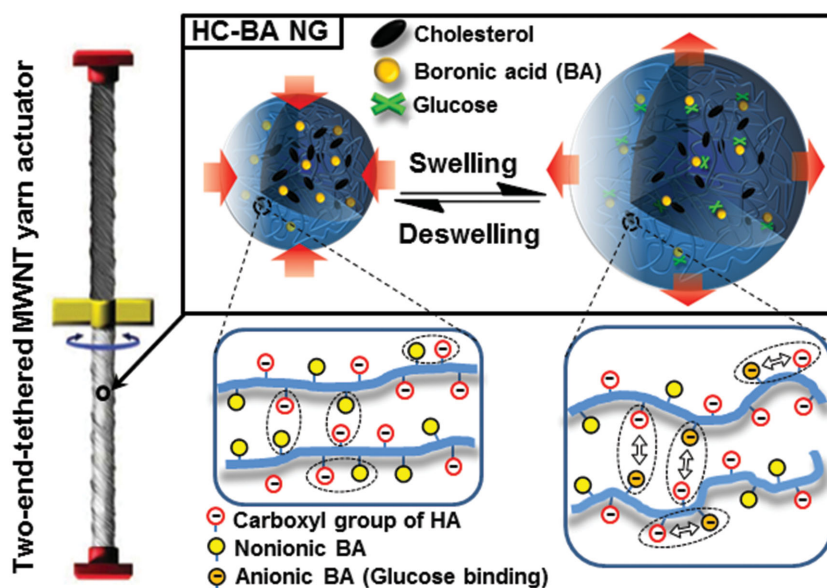
To provide a biologically important sensor–actuator response, we here utilized a nanohydrogel containing a glucose-sensing moiety as guest materials in a MWNT yarn. This guest is a boronic acid-conjugated hyaluronic acid/cholesterol nanogel (HC–BA NG) that reversibly couples, via the BA

Dr. J. Lee, S. Ko, Dr. C. H. Kwon, Prof. S. J. Kim
Center for Self-Powered Actuation
Department of Biomedical Engineering
Hanyang University
222 Wangsimni-ro, Seongdong-gu
Seoul 04763, South Korea
E-mail: sjk@hanyang.ac.kr

Dr. M. D. Lima, Prof. R. H. Baughman
The Alan G. MacDiarmid NanoTech Institute
University of Texas at Dallas
800 West Campbell Road, Richardson, TX 75080, USA

DOI: 10.1002/sml.201503509





Scheme 1. Self-powered MWNT yarn actuator deposited with boronic acid-conjugated hyaluronic acid/cholesterol nanogel (HC-BA NG) for glucose sensing.

substituent, with glucose to provide a mechanically actuating sensor response to glucose (Scheme 1). For the configuration of the torsional actuating yarn, we adopted the two-end-tethered, half-infiltrated homochiral yarn structure described in a previous report.^[17] A volume change in the nanogel, which is infiltrated as guest material in the MWNT yarn, resulted from a glucose-sensitive change in electric charge alteration of the BA, which provided self-powered torsional actuation of the MWNT yarn.

Hyaluronic acid (HA) is a linear anionic glycosaminoglycan with repeating units of D-glucuronic acid and D-N-acetylglucosamine, which is widely distributed in the extracellular matrix and contributes to both structural and biological functions through its ability to interact with other materials.^[18,19] Unlike other synthetic polymers, HA is biocompatible, biodegradable, and nonimmunogenic, and has been widely studied for biomedical and pharmaceutical applications.^[20–22] Recently, various polymeric nanoparticles or NGs using HA have been synthesized and utilized as drug carriers and bioimaging probes^[23,24] However, it is difficult to find the studies of the application of HA as a biosensing actuating material.

There are several advantages of using the NG rather than other cross-linked polymer as a guest material for MWNTs yarns. Hydrogel nanoparticles can sensitively respond to their surrounding environment because of their large surface area and tridimensional structure. Moreover, it is possible to use them for a potential controlled-release system because of their ability to encapsulate specific molecules, such as proteins or other biological components. NGs can also be easily produced by a simple synthetic process and are easy to handle in various applications.

To introduce the reversible glucose-sensing property, we selected the BA-containing compound and conjugated it to the HC NG. BA is known to be highly selective and sensitive for the *cis*-diol on glucose and has reproducible and stable

reversible binding properties.^[8,25,26] There have been many studies of the application of BA for glucose sensing using various methods, including colorimetric, fluorescent, or electrochemical changes, but many problems remain, such as photochemical instability and particular difficulty in electrical connections.^[9,27–30]

We designed compact polymeric nanoparticles of HA (modified by hydrophobic cholesterol and phenylboronic acid) as a guest material for MWNT yarn, and then utilized their reversible swelling/deswelling for yarn actuation.

In the presence of glucose, a critical number of nonionic trigonal BA units in the HA NG become negatively charged tetrahedral boronate esters as a result of their binding to glucose in aqueous media. This causes volumetric expansion of the NG by electrostatic repulsion between negatively charged carboxyl groups of HA and anionic boronates. It

is expected that the NG swelling should be reversed by an overall decrease in the negative charge in the nanoparticle, resulting from the increase in glucose-unbound boron in glucose-reduced conditions. In this paper, we investigated the sensitivity of the swelling property of BA-conjugated NG depending on the surrounding glucose concentration and confirmed the possibility of the biosensing application of artificial muscles using yarn volume change to drive torsional actuation.

2. Results and Discussions

2.1. Synthesis and Characterization of HC NG and HC-BA NG

We prepared amphiphilic HC-BA NG 7 as shown in Figure 1. First, for the synthesis of amphiphilic HC NG, cholesteryl chloroformate 2 was reacted with ethylenediamine 3, and the amine modified cholesterol 4 was obtained after purification. Then, cholesterol-NH₂ 4 was added to HA 1 activated by N-(3-dimethylaminopropyl)-N'-ethylcarbodiimide (EDC) and N-hydroxysulfosuccinimide (sulfo-NHS), resulting in the preparation of HC NG 5. For introducing the property of reversible binding to glucose 8, 3-aminophenylboronic acids 6 were further reacted with the free carboxyl group of NG in the presence of EDC and sulfo-NHS.

The chemical structure of NG and the degree of substitution (DS), defined as the number of conjugated cholesterols per 100 β -glucosamine residues of HA, were analyzed using Proton Nuclear Magnetic Resonance (¹H-NMR). A characteristic peak of cholesteryl chloroformate, the double-bond signal, was confirmed at 5.4 ppm (1H, -CHCH₂-) and ethylenediamine-reacted cholesterol showed specific peaks at 2.8 ppm (2H, -NH₂CH₂) and 3.2 ppm (2H, -NHCH₂-). In the case of HA, a chemical shift of the N-acetyl group (δ = 2 ppm, 3H, -COCH₃) was assigned as the characteristic

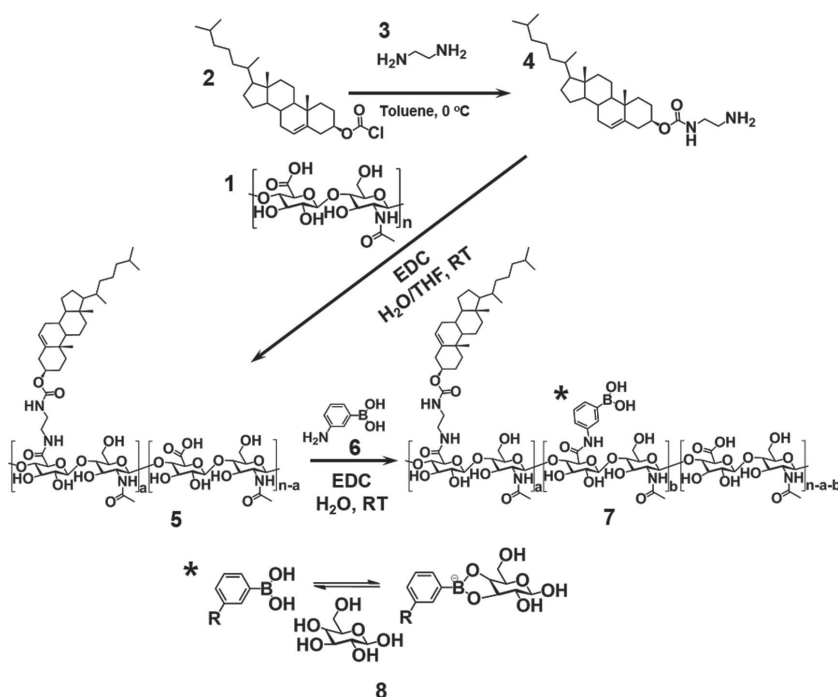


Figure 1. Synthetic process for HC-BA NG. **1.** Hyaluronic acid (HA). **2.** Cholesterylchloroformate. **3.** Ethylenediamine. **4.** Cholesterol-NH₂. **5.** HC NG. **6.** 3-aminophenylboronic acids. **7.** HC-BA NG. **8.** D-(+)-glucose. *. Reversible binding between phenylboronic acid and glucose.

peak. After the reaction between HA and ethylenediamine-conjugated cholesterol, the characteristic peak of cholesterol ($\delta = 5.4$ ppm) was confirmed to be present in the HC NG ¹H-NMR spectrum (see Figure S1 in the Supporting Information). Then, the DS was estimated from the integration ratio between the peaks of cholesterol ($\delta = 5.4$ ppm) and the N-acetyl group in HA ($\delta = 2$ ppm). The DS of the HC NG was determined to be 14.9 mole% when the reaction ratio of cholesterol-NH₂ groups to carboxyl groups in HA was 0.2 (Figure S2, Supporting Information). HC NG was further reacted with 3-aminophenylboronic acid, and the presence of the phenylboronic acid moiety in the final product, HC-BA NG, was also clearly confirmed by Fourier Transform Infrared Spectroscopy (FT-IR) analysis (Figure S3, Supporting Information).

The critical micelle concentration (CMC) of HC NG was measured in the presence of a pyrene fluorescence probe. The amphiphilic nature of the HC NG, consisting of hydrophobic cholesterol and hydrophilic HA, results in micelle formation in aqueous solution, and these micelles of HC NG can be evaluated using a fluorescence probe technique. From the excitation spectra of pyrene in the HC NG solution at various concentrations, the CMC was determined by plotting the ratio of intensities at wavelengths of 338 and 333 nm versus the concentration of HC NG, and the CMC of the sample was calculated to be ≈ 0.006 mg mL⁻¹ (Figure S4, Supporting Information). The synthesized HC NG and HC-BA NG were dispersed in phosphate-buffered saline (PBS) buffer (pH 7.4) and their particle sizes and morphologies were analyzed using dynamic light scattering (DLS). The hydrodynamic size of HC NG was determined to be ≈ 250 nm (Figure S5, Supporting Information).

2.2. Swelling Properties of HC NG and HC-BA NG

Previously, the swelling ratio of the hydrogel has been calculated from the differences in film thickness.^[31] However, in this paper, the weights of the NGs were used for the calculation instead of the hydrogel thickness, and the swelling ratio of NG was obtained using the following equation (1)

$$\text{Swelling ratio (\%)} = \frac{(\text{Swollen weight} - \text{Dried weight})}{\text{Dried weight}} \times 100\% \quad (1)$$

As shown in **Figure 2A**, dried HC-BA NG rapidly absorbed water for 10 min and was saturated to $\approx 180\%$ swelling after 2 h. This NG was then immersed in 5×10^{-3} , 10×10^{-3} , and 20×10^{-3} M glucose solution (Figure 2B), resulting in an increase of the swelling ratio to 200–230% after 40 min. The change in size of the glucose-sensitive particles of HC-BA NG was also confirmed by DLS analysis (Figure 2C). The particle

size of HC-BA NG in PBS buffer without glucose was around 300 nm, but the size increased to ≈ 1 μ m after the addition of glucose to the PBS (final conc. = 100×10^{-3} M). In the control experiment, HC NG without BA also showed a volume expansion in PBS, but there was no difference in its swelling in the presence of glucose (Figure 2D). These results support the hypothesis that a critical number of nonionic trigonal boronate esters as a result of binding to diols of glucose, allowing the NG to be volumetrically expanded by electrostatic repulsion at physiological pH between the negatively charged carboxyl groups of HA and anionic boronate.

2.3. MWNT Yarn Artificial Muscle Actuator Deposited with HC-BA NG

Then, HC-BA NG was introduced as a guest material of the MWNT yarn, and a torsional yarn actuator was fabricated as a homochiral structure that supported a paddle, as previously described.^[17,32] **Figure 3** illustrates the process of A) HC-BA NG formation, B) images of the nanoparticle morphology (transmission electron microscopy (TEM)), and C) MWNT yarn (scanning electron microscopy (SEM)). Cholesterol-conjugated HA can easily form spherical nanoparticles, HC NG, with an outer hydrophilic backbone of HA and an inner accumulation of hydrophobic cholesterol. Phenylboronic acids were further conjugated to this NG as a glucose-sensing moiety (Figure 3A). As shown in the TEM image (Figure 3B), HC-BA NG clearly forms spherical nanoparticles with a diameter of ≈ 200 to ≈ 250 nm. In the SEM images of the MWNT yarn (Figure 3C), the thickness of the

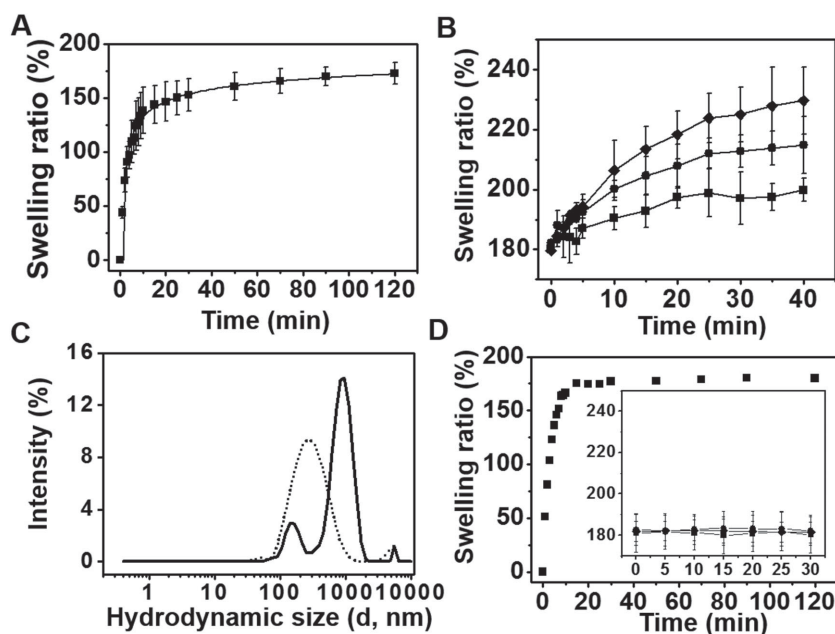


Figure 2. Swelling properties of NGs. A) Time-dependent swelling of HC-BA NG pellet in $1 \times$ PBS buffer. B) HC-BA NG pellet swelling in different glucose concentrations: 20×10^{-3} M (\bullet), 10×10^{-3} M (\circ), and 5×10^{-3} M (\blacksquare). C) Hydrodynamic size, measured by dynamic light scattering, of HC-BA NG in PBS buffer with (solid line) and without (dashed line) 100×10^{-3} M glucose. D) Swelling of HC NG in PBS and in the presence of glucose (inset graph, Control). A,D) For the swelling test, dried NG pellet was directly immersed in PBS buffer and the swelling ratio was calculated by measuring the weight of NG after 120 min. After 2 h incubation of hydrogel in PBS buffer, the swelling ratio in the presence of B) different glucose concentrations (5×10^{-3} , 10×10^{-3} , and 20×10^{-3} M, inset graphs in panel D)) was obtained. All samples were measured three times at room temperature.

bare yarn was $\approx 30 \mu\text{m}$ with $\approx 20^\circ$ helix angle (α) (Figure 3C upper) and HC-BA NG-deposited yarn showed a thickness of $\approx 40 \mu\text{m}$ with $\approx 40^\circ$ helix angle (α') in the same twisted-yarn

help ensure reversible torsional actuation, we used a two-end-tethered structure (Scheme 1) with a lower guest-filled yarn segment acting as a torsional actuator and an upper

condition (Figure 3C lower). This image also clearly shows that the HC-BA NGs were homogeneously loaded onto the MWNT yarn without any noticeable mismatches, such as grains, strains, or cracks.

For measuring the loading efficiency of HC-BA NG, the loading mass of HC-BA NGs onto MWNT was analyzed by comparing with bare MWNT weight. Average weight of bare MWNT yarn obtained from $1.0 \times 7.5 \text{ cm}^2$ sized three-layer MWNT sheet was $30.7 \mu\text{g}$ and that of HC-BA NGs deposited MWNT yarn was $1095.1 \mu\text{g}$. The loading efficiency of NGs was calculated by following equation (2)

$$\text{Loading efficiency (\%)} = \frac{\text{Weight of NGs in MWNT yarn}}{\text{Weight of NGs and MWNT yarn}} \times 100\% \quad (2)$$

According to the above equation, HC-BA NGs showed 97.2% of loading efficiency and this result suggests that the HC-BA NGs are highly compatible with MWNT yarn.

Evaluation of torsional actuation of the guest-containing MWNT yarn was performed in a PBS buffer flow system in which various glucose concentrations were provided using a peristaltic pump (Figure S6, Supporting Information). To

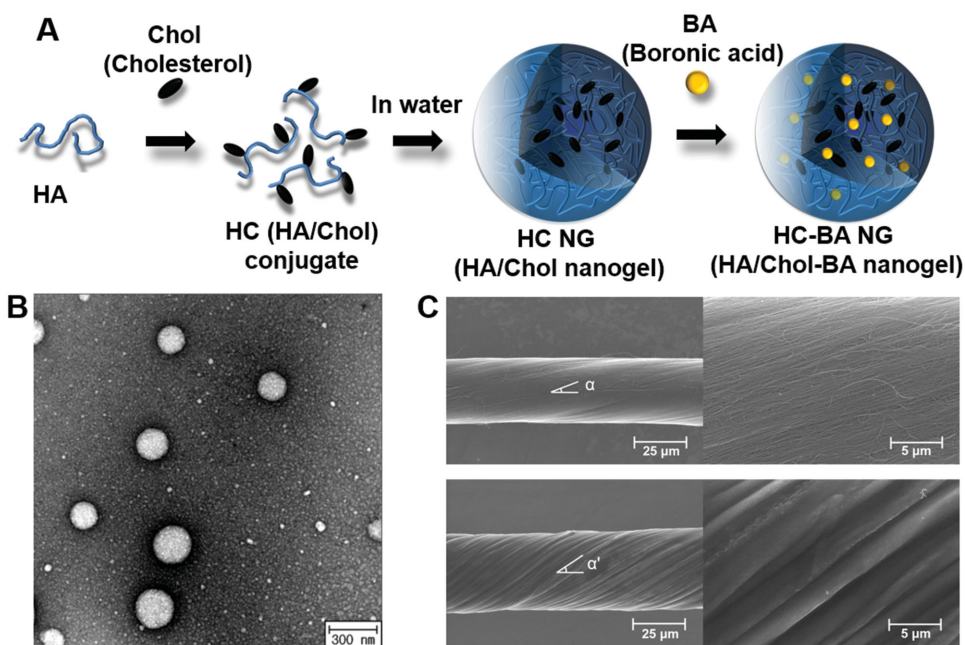


Figure 3. A) HC-BA NG formation. B) Transmission electron microscopy (TEM) image of HC-BA NG. C) Scanning electron microscopy (SEM) images of two-end-tethered homochiral yarn actuator muscle segments: Neat MWNT yarn (upper) and HC-BA NG-coated yarn (lower) at low magnification (left) and high magnification (right).

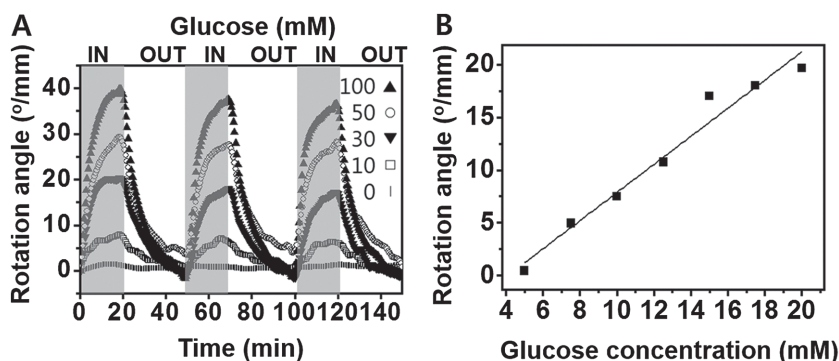


Figure 4. A) Reversible torsional actuation of HCNG-BA deposited MWCNT yarn depending on the glucose concentration. B) Actuation depending on different glucose concentration.

guest-free yarn segment functioning as a torsional spring to return the paddle to its starting angle.^[32]

Reversible paddle rotation in PBS buffer, depending upon glucose concentration in the buffer, resulted from the swelling/deswelling property of HC-BA NGs embedded within the yarn. The degree of rotation of the actuator was obtained from a movie of the paddle rotation (see Movie, Supporting Information). As shown in **Figure 4A**, measured rotation angles (expressed as degree paddle rotation per yarn length in mm) varied from $\approx 10^\circ \text{ mm}^{-1}$ (at $10 \times 10^{-3} \text{ M}$ glucose) to $\approx 40^\circ \text{ mm}^{-1}$ (at $100 \times 10^{-3} \text{ M}$ glucose), and the paddle rotation angle was reversed to the starting position when the glucose was removed. After addition of the glucose-containing buffer, the paddle rotated in the untwisting direction for the actuating yarn segment and stopped after 20 min. When the glucose-containing buffer was replaced by glucose-free buffer, the direction of paddle rotation was reversed and the final rotation angle was achieved in about 30 min. This result suggests that this actuator can be applied as a reversible self-powered actuating glucose sensor having a short response time compared with previous reports.^[33]

Figure 4B shows a graph of paddle rotation angle versus glucose concentration. This shows that the rotation angle increased linearly from 0° to $\approx 20^\circ$ in the presence of glucose concentrations between 5×10^{-3} and $20 \times 10^{-3} \text{ M}$. These results suggest that the glucose-sensing properties of the MWNT yarn torsional actuator could be applied in drug delivery devices in which the extent of torsional actuation controls drug delivery. Importantly, the torsional actuation angle realized precisely responds to glucose concentration within the concentration range needed to monitor normal human glucose levels (below $5.6 \times 10^{-3} \text{ M}$ before eating and $7.8 \times 10^{-3} \text{ M}$ two hours after eating) and abnormal human glucose levels (above $7.0 \times 10^{-3} \text{ M}$ before eating and $11.1 \times 10^{-3} \text{ M}$ two hours after eating).^[34]

3. Conclusion

We developed a bioactuating MWNT yarn artificial muscle by using the reversible volume expansion of a glucose-sensitive guest hydrogel, HC-BA NG. After incorporation of HC-BA NG within the twist-spun MWNT yarn, we fabricated a two-end-tethered torsional actuator. Then, we demonstrated

reversible torsional actuation of the MWNT artificial muscle that depended sensitively on glucose concentration in the range of 5×10^{-3} – $100 \times 10^{-3} \text{ M}$. These results suggest that this biosensing yarn might eventually be deployable as an implantable, self-powered actuating sensor for controlled drug delivery.

4. Experimental Section

Materials: Sodium hyaluronate (HA200K, M_w 213 kDa) was obtained from Lifecore Biomedical (Chaska, MN, USA). Cholesterol chloroformate, ethylenediamine, EDC, sulfo-NHS, 3-aminophenylboronic acid hydrochloride, and D-(+)-glucose were purchased from Sigma-Aldrich (St. Louis, MO, USA). All other chemicals were analytical grade and used as received without any further purification.

Synthesis of Amine Modified Cholesterol: For the preparation of amine-modified cholesterol, cholesterol chloroformate was reacted with ethylenediamine, as previously described.^[35] Briefly, cholesterol chloroformate (2.25 g, 5 mmol) in anhydrous toluene (50 mL) was added dropwise into a solution of ethylenediamine (16.7 mL, 250 mmol) in 150 mL toluene for 10 min at 0°C . After overnight stirring at room temperature, unreacted ethylenediamine was washed out thoroughly with distilled water and the mixture was dried over anhydrous magnesium sulfate. After evaporation of the solvent, the dried mixture was dissolved in 100 mL of dichloromethane/methanol (1/1, v/v) solution and the byproduct was removed with a syringe filter (1 μm MWCO, PTFE, Whatman, NJ, USA). Then, the filtrate was crystallized under rotary evaporation and analyzed by $^1\text{H-NMR}$ (600 MHz, Varian Unity Plus, CA, USA).

Synthesis of HC NG (HA/Cholesterol Nanogel): Amine-modified cholesterol was conjugated through the carboxyl group of HA using the EDC coupling method. Briefly, HA (100 mg, 244 μmol) was solubilized in 10 mL of distilled water. Then, EDC (93.5 mg) and sulfo-NHS (106 mg) were added and the carboxyl moiety of HA was activated for 30 min. Then, amine-modified cholesterol (48.8 μmol) in 10 mL of tetrahydrofuran (THF) were slowly added to the HA solution with stirring, and reacted for 18 h. After the reaction, samples were dialyzed using a cellulose membrane tube (MWCO 12 kDa, Spectrum Laboratories, Inc., CA, USA) in distilled water/THF (1/1, v/v) solution for 2 d, then fresh water for 1 d, and then the sample solutions were solidified by freeze drying. After dissolving the samples in D_2O /THF- d_8 (1/1, v/v) solution, the cholesterol content of the HC NGs was estimated by $^1\text{H-NMR}$ analysis.

Preparation of HC-BA NG (HA/Cholesterol-Boronic Acid Nanogel): The synthesized HC NGs were further reacted with 3-aminophenylboronic acid hydrochloride. Briefly, crystallized HC NGs (20 mg) were redissolved in 10 mL of distilled water and 10 mg of EDC was added with vigorous stirring. Then, 3-aminophenylboronic acid hydrochloride (1 mL of $50 \times 10^{-3} \text{ M}$ in distilled water) was directly added dropwise into the solution and reacted for 12 h. Synthesized HC-BA conjugates were purified by dialysis and recrystallized by freeze drying. The dried HC-BA NG powder was further analyzed by FT-IR (Nicolet iS50, Thermo Fisher Scientific Inc. PA, USA).

Characterization of HC NGs and HC–BA NGs: The particle sizes of HC and HC–BA NGs were measured by DLS. HC NGs and HC–BA NGs (2 mg mL^{-1}) dissolved in PBS buffer (pH 7.4) were sonicated for 2 min using a probe-type sonicator (Branson, MO, USA). Then, after further purification of samples, using a $0.45 \mu\text{m}$ pore size membrane filter, the hydrodynamic sizes of nanoparticles were obtained using a DLS instrument (Zetasizer Nano ZS, Malvern, UK). The surface morphology of HC–BA NG was observed using TEM (Philips CM 200, CA, USA) after negative sample staining with uranyl acetate.

The CMC of HC NG after pyrene addition was also calculated by fluorescence spectroscopy as previously described.^[36,37] Pyrene in acetone ($30 \times 10^{-3} \text{ M}$) was diluted with distilled water to $1.2 \times 10^{-6} \text{ M}$. Then, HC NG at various concentrations from 1 to 0.001 mg mL^{-1} was mixed with pyrene solution at a 1:1 volume ratio. The excitation spectra of pyrene (300–360 nm, emission 390 nm) were obtained using a fluorometer (F-7000, Hitachi High-Technologies Corporation, Tokyo, Japan) and the CMC was determined by plotting the ratio of intensity at wavelengths of 338 and 333 nm versus the HC NG concentration.

Swelling/Deswelling Properties of HC–BA NG Depending on the Environmental Glucose: To determine the swelling characteristics of the HC–BA NG, HC–BA NGs were further induced to condense and aggregate into pellets. 10 mg mL^{-1} of HC–BA NG solution was centrifuged at 30 000 rpm for 30 min and the precipitated NG pellet was dried in a vacuum oven for 12 h. After measuring the initial weight of dried NG pellet, sample was immersed into PBS buffer with different glucose concentration. The weight change of sample was monitored by a balance after wiping the surface water of pellet taken out at appropriate times. All data was obtained using three independent sample sets.

Swelling property of glucose sensitive HC–BA NG was also analyzed by DLS. All samples with/without glucose were sonicated and filtered before the test. Then, swelling degree of nanogels depending on glucose was evaluated from hydrodynamic size distribution.

HC–BA NG Deposited MWNT Yarn Fabrication: A three-layered MWNT sheet was prepared on a glass slide from the MWNT forest. The sheet stack was immersed in HC–BA NG solution and dried at room temperature to attach the NG to the MWNT sheet. The dried sheet was rewetted and one end of the sheet was carefully lifted from the glass slide with an electric motor shaft and twisted into a yarn with ≈ 2100 turns counterclockwise per meter of yarn length. A bare yarn with the same number of turns per meter of yarn length was used as a torsional spring for the artificial muscle.

The two yarns were connected by a paddle (yellow tape, size $0.5 \times 2.0 \text{ mm}$) to form a two-body structure, and the other two ends were tethered to a solid template. The sample was desiccated overnight.

The loading amount of HC–BA NG on MWNT yarn was also measured by ultra-microbalance (XP2U, Mettler Toledo, OH, USA). Three independent sample sets of HC–BA NGs treated yarns were fabricated from same sized three-layered MWNT sheets ($1.0 \times 7.5 \text{ cm}^2$) on glass slide and bare yarns samples without nanogel also were prepared as a control experiment. Then, averaged mean weight of guest HC–BA NGs was obtained by subtraction of bare yarn weight and nanogel loading efficiency was further calculated.

Configuration of Torsional Actuation of MWNT Yarn: Mechanical movement of the MWNT yarn driven by the swelling/deswelling

properties of the hydrogel was observed in a continuous-flow PBS buffer (pH 7.4) system driven by a peristaltic pump (LEAD-2, Baoding Longer Precision Pump Co., Ltd., Hebei, China) at room temperature. Before recording a movie of the torsional actuation, the actuating yarn was immersed in PBS buffer for $\approx 2 \text{ h}$ to stabilize the rotation angle. PBS buffers with different glucose concentrations (0×10^{-3} , 5×10^{-3} , 10×10^{-3} , and $20 \times 10^{-3} \text{ M}$) were prepared and each injected into the system for 20 min. After this, fresh PBS buffer solution was reinjected for 30 min to remove the glucose from the sample. For the sequential glucose concentration change experiment, the solution exchange intervals were 30 min to show the rotation angle of the artificial muscle.

Supporting Information

Supporting Information is available from the Wiley Online Library or from the author.

Acknowledgements

This work was supported by the Creative Research Initiative Center for Self-powered Actuation and the Korea-US Air Force Cooperation Program Grant No. 2013K1A3A1A32035592 in Korea. Support at the University of Texas at Dallas was provided by Air Force Office of Scientific Research grants FA9550-15-1-0089 and AOARD-FA2386-13-4119, NASA grants NNX14CS09P and NNX15CS05C, and the Robert A. Welch Foundation grant AT-0029.

- [1] W. L. Clarke, D. Cox, L. A. Gonderfrederick, W. Carter, S. L. Pohl, *Diabetes Care* **1987**, *10*, 622.
- [2] G. Van den Berghe, P. Wouters, F. Weekers, C. Verwaest, F. Bruyninckx, M. Schetz, D. Vlasselaers, P. Ferdinande, P. Lauwers, R. Bouillon, *N. Engl. J. Med.* **2001**, *345*, 1359.
- [3] R. Ballerstadt, R. Ewald, *Biosens. Bioelectron.* **1994**, *9*, 557.
- [4] D. C. Klonoff, *Diabetes Care* **2005**, *28*, 1231.
- [5] W. Yan, X. Feng, X. Chen, W. Hou, J.-J. Zhu, *Biosens. Bioelectron.* **2008**, *23*, 925.
- [6] A. S. G. Huggett, D. A. Nixon, *Lancet* **1957**, *2*, 368.
- [7] J. Wang, *Chem. Rev.* **2008**, *108*, 814.
- [8] J. P. Lorand, J. O. Edwards, *J. Org. Chem.* **1959**, *24*, 769.
- [9] A. Kikuchi, K. Suzuki, O. Okabayashi, H. Hoshino, K. Kataoka, Y. Sakurai, T. Okano, *Anal. Chem.* **1996**, *68*, 823.
- [10] V. L. Alexeev, S. Das, D. N. Finegold, S. A. Asher, *Clin. Chem.* **2004**, *50*, 2353.
- [11] C. Zhang, G. G. Cano, P. V. Braun, *Adv. Mater.* **2014**, *26*, 5678.
- [12] M. Zhang, K. R. Atkinson, R. H. Baughman, *Science* **2004**, *306*, 1358.
- [13] D. Li, W. F. Paxton, R. H. Baughman, T. J. Huang, J. F. Stoddart, P. S. Weiss, *MRS Bull.* **2009**, *34*, 671.
- [14] A. B. Dalton, S. Collins, E. Munoz, J. M. Razal, V. H. Ebron, J. P. Ferraris, J. N. Coleman, B. G. Kim, R. H. Baughman, *Nature* **2003**, *423*, 703.
- [15] M. D. Lima, S. Fang, X. Lepro, C. Lewis, R. Ovalle-Robles, J. Carretero-Gonzalez, E. Castillo-Martinez, M. E. Kozlov, J. Oh, N. Rawat, C. S. Haines, M. H. Haque, V. Aare, S. Stoughton, A. A. Zakhidov, R. H. Baughman, *Science* **2011**, *331*, 51.

- [16] J. Ren, Y. Zhang, W. Bai, X. Chen, Z. Zhang, X. Fang, W. Weng, Y. Wang, H. Peng, *Angew. Chem., Int. Ed. Engl.* **2014**, *53*, 7864.
- [17] M. D. Lima, N. Li, M. J. de Andrade, S. Fang, J. Oh, G. M. Spinks, M. E. Kozlov, C. S. Haines, D. Suh, J. Foroughi, S. J. Kim, Y. Chen, T. Ware, M. K. Shin, L. D. Machado, A. F. Fonseca, J. D. W. Madden, W. E. Voit, D. S. Galvao, R. H. Baughman, *Science* **2012**, *338*, 928.
- [18] T. C. Laurent, J. R. E. Fraser, *FASEB J.* **1992**, *6*, 2397.
- [19] L. Lapcik, S. De Smedt, J. Demeester, P. Chabreck, *Chem. Rev.* **1998**, *98*, 2663.
- [20] N. Itano, F. Atsumi, T. Sawai, Y. Yamada, O. Miyaishi, T. Senga, M. Hamaguchi, K. Kimata, *Proc. Natl. Acad. Sci. USA* **2002**, *99*, 3609.
- [21] V. Trochon, C. Mabilat, P. Bertrand, Y. Legrand, F. Smadjaoffe, C. Soria, B. Delpech, H. Lu, *Int. J. Cancer* **1996**, *66*, 664.
- [22] J. B. Leach, K. A. Bivens, C. W. Patrick, C. E. Schmidt, *Biotechnol. Bioeng.* **2003**, *82*, 578.
- [23] J. A. Burdick, G. D. Prestwich, *Adv. Mater.* **2011**, *23*, H41.
- [24] K. Y. Choi, H. Chung, K. H. Min, H. Y. Yoon, K. Kim, J. H. Park, I. C. Kwon, S. Y. Jeong, *Biomaterials* **2010**, *31*, 106.
- [25] F. Horkay, S. H. Cho, P. Tathireddy, L. Rieth, F. Solzbacher, J. Magda, *Sens. Actuators, B* **2011**, *160*, 1363.
- [26] W. Q. Yang, X. M. Gao, B. H. Wang, *Med. Res. Rev.* **2003**, *23*, 346.
- [27] T. D. James, K. Sandanayake, S. Shinkai, *Angew. Chem., Int. Ed. Engl.* **1994**, *33*, 2207.
- [28] J. N. Cambre, B. S. Sumerlin, *Polymer* **2011**, *52*, 4631.
- [29] J. T. Suri, D. B. Cordes, F. E. Cappuccio, R. A. Wessling, B. Singaram, *Angew. Chem., Int. Ed. Engl.* **2003**, *42*, 5857.
- [30] C. J. Ward, P. Patel, T. D. James, *J. Chem. Soc., Perkin Trans. 1* **2002**, *1*, 462.
- [31] M. D. Miller, M. L. Bruening, *Chem. Mater.* **2005**, *17*, 5375.
- [32] J. Foroughi, G. M. Spinks, G. G. Wallace, J. Oh, M. E. Kozlov, S. Fang, T. Mirfakhrai, J. D. W. Madden, M. K. Shin, S. J. Kim, R. H. Baughman, *Science* **2011**, *334*, 494.
- [33] G. Lin, S. Chang, H. Hao, P. Tathireddy, M. Orthner, J. Magda, F. Solzbacher, *Sens. Actuators, B* **2010**, *144*, 332.
- [34] A. Am Diabetes, *Diabetes Care* **2006**, *29*, S4.
- [35] T. Ishi-i, R. Iguchi, E. Snip, M. Ikeda, S. Shinkai, *Langmuir* **2001**, *17*, 5825.
- [36] G. B. Ray, I. Chakraborty, S. P. Moulik, *J. Colloid Interface Sci.* **2006**, *294*, 248.
- [37] L. Wang, R. Zeng, C. Li, R. Qiao, *Colloids Surf., B* **2009**, *74*, 284.

Received: November 17, 2015
Revised: January 20, 2016
Published online: March 1, 2016